

Broadband Phase-to-Intensity Modulation Conversion for Microwave Photonics Processing Using Brillouin-Assisted Carrier Phase Shift

Wei Li, Ning Hua Zhu, *Member, IEEE*, Li Xian Wang, and Hui Wang

Abstract—We theoretically and experimentally demonstrate a novel broadband phase-to-intensity modulation conversion technique for microwave photonics processing system. The technique is based on optical carrier phase shift of a phase modulated signal using stimulated Brillouin scattering. More than 360° carrier phase shift can be achieved. By simply adjusting the carrier phase shift while preserving its amplitude unchanged, the phase modulation can be fully or partially converted to intensity modulation. The main advantage of the proposed method lies in its broadband nature since the SBS is only imparted on the optical carrier and the phase modulated sidebands are not affected as long as the modulating frequency is higher than the Brillouin bandwidth. In addition, as a microwave photonics processing application, we demonstrate the dispersion induced power penalty control in radio-over-fiber systems using the proposed technique. Experimental results match well with the theoretical prediction.

Index Terms—Phase-to-intensity modulation conversion, stimulated Brillouin scattering, radio-over-fiber.

I. INTRODUCTION

OPTICAL phase modulation has attracted great interest in microwave photonics processing systems, such as photonic microwave filters [1]–[3], radio-over-fiber (RoF) systems [4], [5], instantaneous microwave frequency measurement [6], optical microwave signal generation [7], [8], subcarrier frequency upconversion [9], and photonic generation of ultrawideband (UWB) signals [10], [11]. The main advantage of using an optical phase modulator (PM) in the microwave photonics processing systems is that the PM is free from the dc bias-drifting problem which exists in an intensity modulated Mach-Zehnder modulator (MZM) based system. In addition, the PM is simpler and has smaller insertion loss. The intensity modulated signal can be directly detected using a photodetector (PD). However, the phase modulated signal has a constant envelope which cannot be directly detected by the PD. Although in the PD the phase modulated sidebands beat with each other and beat with the optical carrier, they produce no beat signal.

Manuscript received July 26, 2011; revised October 03, 2011; accepted October 15, 2011. Date of publication October 25, 2011; date of current version November 30, 2011. This work was supported by the National Natural Science Foundation of China under Grants 61108002, 61127018, 61021003, 61177060, 61090390, 61177080, and 60820106004.

The authors are with the State Key Laboratory on Integrated Optoelectronics, Institute of Semiconductors, Beijing 100083, China (e-mail: liwei05@semi.ac.cn).

Color versions of one or more of the figures in this paper are available online at <http://ieeexplore.ieee.org>.

Digital Object Identifier 10.1109/JLT.2011.2173462

For each beat signal there is always another beat signal which has the same frequency and amplitude but opposite phase. They will cancel each other out perfectly [7]. In order to recover the information that is carried by the optical phase, the phase modulated signal should be converted to an intensity modulated signal.

The coherent detection method based on heterodyne or homodyne scheme can be used to realize phase-to-intensity modulation conversion, where the phase modulated signal is made to beat with a local oscillator light. However, it is difficult to build a local-oscillator light source with its phase that is locked to the signal light source [10]. In addition, this method is very sensitive to the environmental influence, which would lead to noise after photodetection.

The other commonly used method is to break the perfect balance among the phase modulated sidebands by modifying their phases or amplitudes. In [9], [12], a dispersive device is used to change the phase relationship between the sidebands. In [10], [13], an optical filter is employed to act as an optical frequency discriminator to introduce different loss to the phase modulated sidebands. In [7], SBS is used to selectively amplify one of the phase modulated sidebands. By using these methods, phase-to-intensity modulation conversion can be realized since the perfect balance among the phase modulated sidebands is broken. However, the techniques based on dispersive device, such as dispersive fiber, cannot be used to implement broadband microwave signal processing since the dispersion-induced phase shift is frequency-dependent. Moreover, for a fixed length optical fiber, the frequencies of the microwave signals should be changed in order to avoid chromatic dispersion-induced power penalty [14]. The method using optical filter as frequency discriminator is restricted by the limited bandwidth of filter slope and the roll-off property of the filter. The operation bandwidth of the SBS-based phase-to-intensity conversion is limited to several tens of megahertz due to the narrow bandwidth of the SBS interaction.

In this paper, we present a novel broadband phase-to-intensity modulation conversion technique for microwave photonics processing systems based on SBS. To the best of our knowledge, this is the first time that the Brillouin-assisted carrier phase shift is used to realize broadband phase-to-intensity modulation conversion. Compared with approaches in [7], [9], [10], [12], [13] where the phase or amplitude of the phase modulated sidebands are modified to break the perfect balance among them, the key difference of the proposed method is that we change the optical carrier phase of the phase modulated signal while preserving the

amplitude of the optical carrier unchanged instead of modifying the phase or amplitude of the sidebands. In this way, the phase modulation can be fully or partially converted to intensity modulation. The main advantage of the proposed method lies in its broadband nature because the SBS is only imparted on the optical carrier and the phase modulated sidebands are not affected as long as the modulating frequency is higher than the Brillouin bandwidth.

In addition, as a microwave photonics processing application, we demonstrate the dispersion induced power penalty control in RoF systems using the proposed technique. Experimental results match well with the theoretical prediction. The paper is organized into four sections. Following this introductory section, the principle of the proposed technique is described in Section II. Section III shows the experiments and results. Finally, the conclusions and discussions are present in Section IV.

II. PRINCIPLE

We consider that a sinusoidal tone microwave signal with frequency of f_m is modulated on an optical carrier via an optical PM. The electrical field of the phase modulated optical carrier is given by [10]

$$\begin{aligned} E_{PM} &= E_c \exp[j\beta_{PM} \cos(2\pi f_m t)] \\ &= E_o \sum_{n=-\infty}^{n=\infty} j^n J_n(\beta_{PM}) \exp[j2\pi(f_c + n f_m t)] \quad (1) \end{aligned}$$

where E_c is the electrical field of the optical carrier with frequency of f_c and amplitude of E_o , β_{PM} is the phase modulation index, $J_n(\cdot)$ is the Bessel function of the first kind of order n . Under small-signal conditions, only the first-order sidebands are considered and (1) can be simplified as

$$\begin{aligned} E_{PM} &= E_o \{ J_1 \exp[j2\pi(f_c - f_m)t + j\pi/2] \\ &\quad + J_0 \exp(j2\pi f_c t) \\ &\quad + J_1 \exp[j2\pi(f_c + f_m)t + j\pi/2] \} \quad (2) \end{aligned}$$

where $J_1 = -J_{-1}$ is used. To recover the microwave signal, the phase modulated signal should be converted to the intensity modulated signal. In our scheme, to achieve the phase-to-intensity modulation conversion, SBS is used to impart a phase shift to the optical carrier.

Fig. 1 illustrates the principle behind the proposed technique, which is based on counterpropagating a phase modulated optical carrier and two pump signals (pump1 and pump2) in a length of dispersion shifted fiber (DSF). DSF instead of a standard single mode fiber (SMF) is employed to reduce the chromatic dispersion in the SBS process since the dispersion will generate a frequency dependent phase-to-intensity modulation conversion and power penalty [10], [14].

We assume that the two pump signals have the same optical power and frequency interval f_p with respect to the optical carrier as shown in Fig. 1. f_p is chosen to be close to the Brillouin frequency shift (v_B) of the DSF. Therefore, SBS interaction

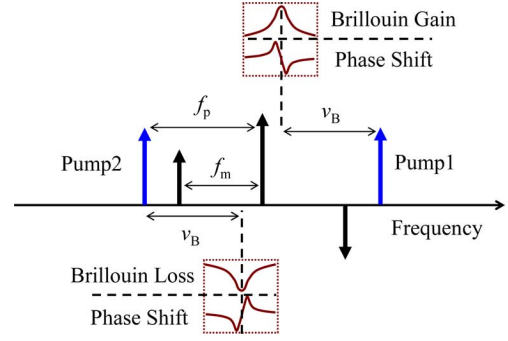


Fig. 1. Principle of the broadband phase-to-intensity modulation conversion based on SBS-induced carrier phase shift. The Brillouin gain/loss and phase shift spectra are also shown. v_B is the Brillouin frequency shift of the optical fiber, f_m is the modulating frequency fed to the PM, and f_p is the frequency interval between the pump wave and optical carrier.

takes place between the optical carrier and the two pump signals. Since the bandwidth of the SBS interaction is very narrow (about several tens of megahertz), the SBS is only imparted on the optical carrier as long as the modulating frequency f_m is higher than the Brillouin bandwidth. In the SBS process, not only the amplitude but also the phase of optical carrier is modified. After the SBS interaction, (2) can be expressed as

$$\begin{aligned} E_{PM} &= E_o J_1 \exp[j2\pi(f_c - f_m)t + j\pi/2] \\ &\quad + E_o A_1 A_2 J_0 \exp[j2\pi f_c t + j(\varphi_1 + \varphi_2)] \\ &\quad + E_o J_1 \exp[j2\pi(f_c + f_m)t + j\pi/2] \quad (3) \end{aligned}$$

where A_1 and A_2 are the amplitude gain generated by pump 1 and pump 2, respectively. φ_1 and φ_2 are the optical phase shift imparted on the optical carrier by pump 1 and pump 2, respectively. The amplitude gain A_n ($n = \pm 1$) is given by [15]

$$A_n = \exp\left(\frac{g_B P_p L_{\text{eff}}}{A_{\text{eff}}} - \alpha L_0\right) \quad (4)$$

where P_p , the pump power, L_{eff} , the effective fiber length, A_{eff} , the effective core area, α , the fiber loss, and L_0 , the fiber length. It should be note that the amplitude gain A_n can also represent Brillouin loss induced by pump 2 by a negative gain coefficient. The SBS gain coefficient is given by [15]

$$g_B = g_o \frac{\Gamma_B^2}{4v_n^2 + \Gamma_B^2} \quad (5)$$

where Γ_B is the full width at half maximum (FWHM) Brillouin linewidth and v_n is the frequency detuning of the optical carrier from the Brillouin resonance. The maximum gain coefficient g_o is given by

$$g_o = \frac{2\pi n^7 p_{1,2}^2 \gamma P_p L_{\text{eff}}}{c \lambda^2 \rho_0 v_a \Gamma_B A_{\text{eff}}} \quad (6)$$

with n the index of refraction, ρ_0 the specific density, v_a the acoustic velocity, $p_{1,2}$ the elasto-optic coefficient, λ the wavelength, c the light speed in vacuum, and $\gamma = 0.5$ for non-po-

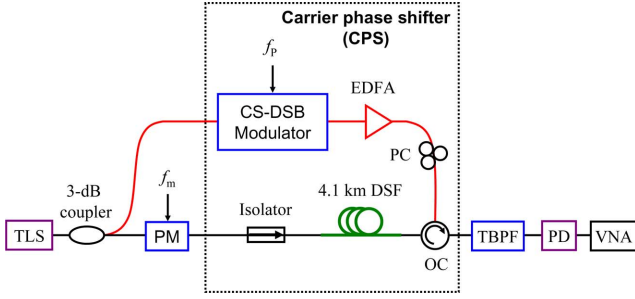


Fig. 2. Experimental setup for investigating broadband phase-to-intensity modulation conversion using SBS-induced carrier phase shift (TLS: tunable laser source; PM: phase modulator; CS-DSB Modulator: carrier suppressed-double sideband modulator; EDFA: erbium-doped fiber amplifier; PC: polarization controller; DSF: dispersion shifted fiber; OC: optical circulator; TBPF: tunable bandpass filter; PD: photodetector; VNA: vector network analyzer).

larization-maintaining fibers. The Brillouin-induced phase shift can be expressed as

$$\varphi_n = g_o \frac{\Gamma_B v_n}{4v_n^2 + \Gamma_B^2} \quad (7)$$

In our case, $g_o(\text{gain}) = -g_o(\text{loss})$, and $v_{+1} = -v_{-1}$. As a result, we have $A_{+1}A_{-1} = 1$ (normalized value) and $\varphi_1 = \varphi_2 = \varphi/2$. Therefore, the optical carrier experiences both Brillouin gain and loss simultaneously. The amplitude of the optical carrier remains almost unchanged because the gain and loss for the optical carrier is mutually canceled out, while the associated optical phase shift imparted on the optical carrier is doubled [16], [17]. Then, (3) can be expressed as

$$E_{\text{PM}} = E_o J_1 \exp[j2\pi(f_c - f_m)t + j\pi/2] + E_o J_0 \exp(j2\pi f_c t + j\varphi) + E_o J_1 \exp[j2\pi(f_c + f_m)t + j\pi/2]. \quad (8)$$

It is interesting to note that the phase modulation is fully converted to intensity modulation under $\varphi = (k + 1/2)\pi$, where k is an integer. When $k\pi < \varphi < (k + 1/2)\pi$, the phase modulation is partially converted to intensity modulation.

III. EXPERIMENTS

In this section, we present the proof-of-concept experiments of the proposed method and apply it for dispersion induced power penalty control in RoF systems.

A. Broadband Phase-to-Intensity Modulation Conversion

Fig. 2 depicts the experimental setup for investigating broadband phase-to-intensity modulation conversion using SBS-induced carrier phase shift. It consists of two main building blocks to perform carrier phase shifter (CPS). The lower part is used to generate phase modulated signal by a PM and stimulate the SBS in a length of DSF while the upper part of the diagram is dedicated to prepare and deliver a carrier suppressed-double sideband (CS-DSB) modulated pump signal required for the implementation of CPS. The two sidebands of the CS-DSB modulated signal act as the two pump signals (pump 1 and pump

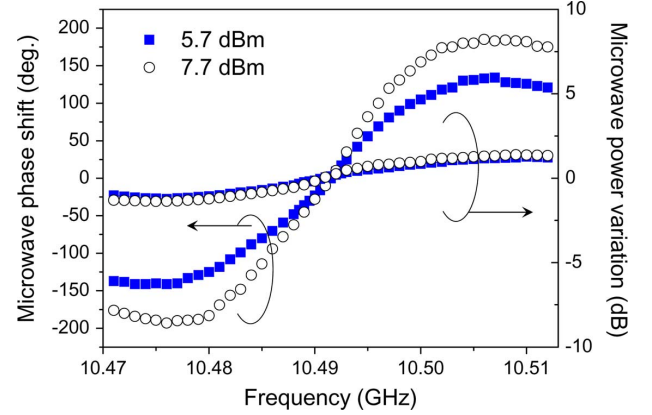


Fig. 3. Measured phase shift and the power variation of the 9 GHz microwave signal as a function of the frequency of f_p for pump power of 5.7 and 7.7 dBm, respectively.

2) as discussed in Section II. In order to avoid the dc bias-drifting problem existed in MZM, the CS-DSB modulation in the upper path can be realized by a PM followed by a Brillouin-assisted notch filter which is used to suppress the optical carrier as demonstrated in [8]. Unfortunately, only one PM was available in our laboratory. Instead of that, a MZM biased at null point was used to generate the CS-DSB modulated signal for a proof-of-concept demonstration in our experiment.

The optical carrier from a commercial tunable laser source (TLS) emitting at $\lambda_c = 1549.945$ nm was split into two branches by a 3-dB optical coupler. In the lower branch, the optical carrier was externally modulated by the PM which was driven by the microwave signal f_m from a vector network analyzer (VNA). An optical isolator was added to ensure unidirectional transmission. The upper path went to an intensity modulator which was driven by the microwave signal of frequency f_p and biased at null point to generate the CS-DSB signal. In addition, f_p was chosen to be close to the Brillouin frequency shift of the DSF. The CS-DSB signal was then boosted using an erbium-doped fiber amplifier (EDFA). An optical circulator (OC) was used to counterpropagate the phase modulated and CS-DSB pump signals in a 4.1 km DSF. In the DSF, the upper and lower sidebands of the CS-DSB pump signal generate Brillouin gain and loss resonances, respectively, with nearly identical depth and spectral shape. Therefore, the amplitude of the optical carrier remains almost constant because the gain and loss for the optical carrier is mutually canceled out, while the associated optical phase shift imparted on the optical carrier is doubled [16], [17]. A polarization controller (PC) was used to optimize the polarization state in the SBS process.

In order to assess the phase shift and amplitude variation introduced to the optical carrier by the SBS, we added a tunable bandpass filter (TBPF) after the OC to block the upper frequency sideband of the phase modulated DSB signal as shown in Fig. 2. A 45 GHz PD was used to convert the optical signal to electrical signal. The phase and power of the microwave signal were measured using the VNA.

Fig. 3 shows the measured phase shift and the power variation of the 9 GHz microwave signal as a function of the frequency of

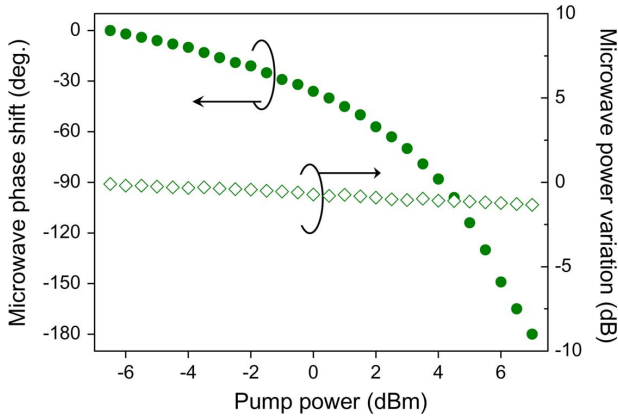


Fig. 4. Measured phase shift and the power variation of the 9 GHz RF signal as a function of the pump power when f_p is fixed at 10.475 GHz.

f_p for pump power of 5.7 and 7.7 dBm, respectively. A continuous phase shift of more than 360° is achieved with pump power of 7.7 dBm. The microwave power variation is less than 3 dB for pump power of 5.7 and 7.7 dBm when the frequency of f_p varies from 10.471 to 10.512 GHz. The microwave power fluctuation can be mainly attributed to the non-perfectly Lorentzian Brillouin shape of the actual SBS spectrum [17]. Fig. 4 highlights another way to adjust the phase of the microwave signal by fixing the frequency of f_p at 10.475 GHz and tuning the optical power of the CS-DSB pump signal. Note that the optical carrier phase shift is equal to that of the microwave signal of 9 GHz because the lower frequency sideband was not affected in the SBS process.

The key advantage of the proposed phase-to-intensity modulation conversion technique lies in its broadband nature. In order to address this point, the frequency of the modulating signal f_m was swept from 7 to 15 GHz while the optical power of the pump signal was fixed at 7.7 dBm. Fig. 5 shows the frequency independent phase shift and power variation of the microwave signal. Nine different traces were measured for frequencies of f_p from 10.481 to 10.502 GHz. Operation of the phase shifts from 7 to 15 GHz were restricted by the limited bandwidth of the TBPF and the PM.

According to (6) and (7), the Brillouin phase shift is also dependent on the wavelength. In fact, the Brillouin frequency shift, ν_B , also varies with the wavelength. Therefore, it allows the use of the TLS to modify the phase of optical carrier without tuning f_p [17].

B. Dispersion Induced Power Penalty Control in RoF Systems

In RoF systems, the DSB modulation is conventionally used to modulate the microwave signal onto the optical carrier. However, it suffers from the well-known power fading effect induced by the fiber dispersion in RoF links [14]. Next, as a microwave photonics processing application, we demonstrate the dispersion induced power penalty control in RoF systems using the proposed technique.

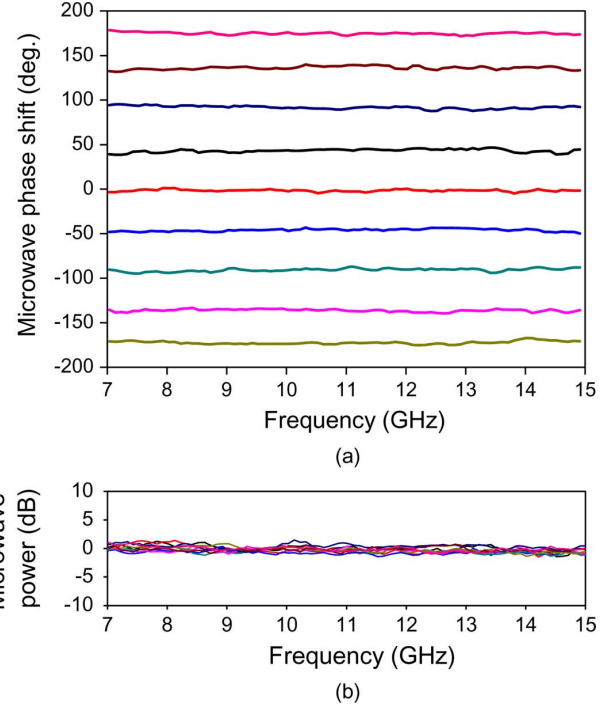


Fig. 5. Frequency independent (a) phase shift and (b) power variation of the microwave signal. Nine different traces were measured for frequencies of f_p from 10.481 to 10.502 GHz under fixed pump power of 7.7 dBm.

The transfer function of the dispersive fiber link is given by

$$H(j2\pi f_m) = \exp\left(\frac{j\pi\lambda_c^2 DL f_m^2}{c}\right) \quad (9)$$

where L is the length of fiber with dispersion D , λ_c is the wavelength of the optical carrier. The complex amplitude of the signal, as previously described by (8), after experiencing the dispersive fiber can be expressed as

$$E_{\text{out}} = E_o \{ J_1 \exp[j2\pi(f_c - f_m)t + j\pi/2] \exp(j\pi\lambda_c^2 DL f_m^2/c) + J_0 \exp(j2\pi f_0 t + j\varphi) + J_1 \exp[j2\pi(f_c + f_m)t + j\pi/2] \exp(j\pi\lambda_c^2 DL f_m^2/c) \}. \quad (10)$$

Then, the microwave power after the PD is proportional to

$$P_m \propto \sin^2(\pi\lambda_c^2 DL f_m^2/c - \varphi). \quad (11)$$

Equation (11) shows that the microwave power penalty is determined by both the link dispersion and the phase shift of the optical carrier. When $\varphi = 0$, it has the same transfer function as the conventional phase modulation dispersive link [6].

In our scheme, the dispersion-induced power penalty can be easily controlled by adjusting the optical carrier phase shift φ .

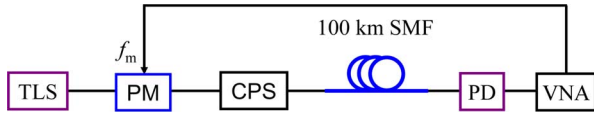


Fig. 6. Experimental setup for investigating the dispersion induced power penalty control in RoF systems using the proposed phase-to-intensity modulation conversion technique (TLS: tunable laser source; PM: phase modulator; CPS: carrier phase shifter; SMF: single-mode fiber; PD: photodetector; VNA: vector network analyzer).

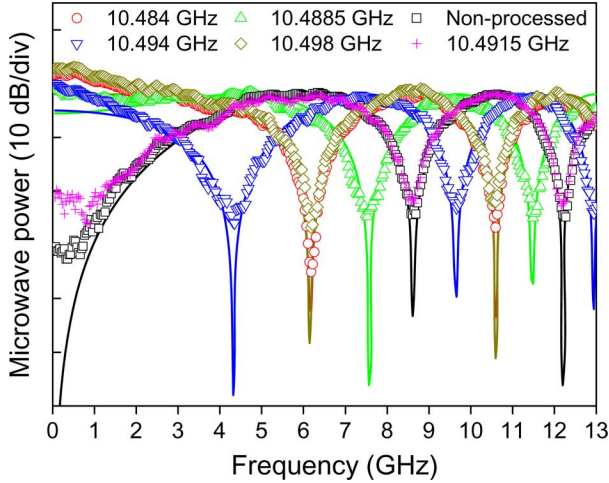


Fig. 7. Measured 100 km SMF link frequency response for the non-processed case and for different frequencies of f_p at the fixed pump power of 5.7 dBm using SBS. Symbols, experimental results; solid curves, theoretical results obtained for $\lambda_c = 1549.945$ nm, and $D = 17$ ps/nm/km.

The maximum transfer of microwave signal f_m requires the carrier phase shift φ to satisfy

$$\varphi = \pi \lambda_c^2 D L f_m^2 / c - (k\pi + \pi/2). \quad (12)$$

It should be noticed that a 180° carrier phase shift is enough to compensate any dispersion induced power penalty.

The experimental setup for investigating the dispersion induced power penalty control in RoF systems is outlined in Fig. 6. The setup comprises the TLS externally modulated with the PM; the CPS, where the phase of the optical carrier can be adjusted (see Fig. 2); and a 100 km SMF, followed by the PD and VNA.

Fig. 7 shows the measured 100 km SMF link frequency response for the non-processed case and for different frequencies of f_p at the fixed pump power of 5.7 dBm using SBS. The figure also shows the results obtained from the theoretical model, which exhibits an excellent agreement with the measured data. It can be seen that the dispersion induced power penalty can be controlled by modifying the phase shift of the optical carrier. For $f_p = 10.484$ and 10.498 GHz, the carrier phase shifts φ are $-\pi/2$ and $\pi/2$, respectively. In both cases, the phase modulation is fully converted to the intensity modulation and the frequency response of the SMF link is the same as that generated by the MZM-based RoF system [14].

IV. CONCLUSION

We have theoretically and experimentally demonstrated a novel broadband phase-to-intensity modulation conversion

technique for microwave photonics processing systems. The technique is based on Brillouin-assisted carrier phase shift of a phase modulated signal. By simply adjusting the phase shift of the optical carrier while preserving its amplitude unchanged, the phase modulation can be fully or partially converted to intensity modulation.

In addition, as a microwave photonics processing application, we have demonstrated the dispersion induced power penalty control in RoF systems. In this application, a 180° carrier phase shift is enough to compensate any dispersion power penalty. Experimental results match well with the theoretical prediction. The main advantage of the proposed method lies in its broadband nature because the SBS is only imparted on the optical carrier and the phase modulated sidebands are not affected as long as the modulating frequency is higher than the Brillouin bandwidth. Therefore, the proposed approach works for broadband microwave frequencies as low as the Brillouin bandwidth to arbitrarily high frequencies, which is only limited by the bandwidth of the optical transmitter and receiver employed. However, there is the other case should be avoided, i.e., $f_m \sim 21$ GHz ($2 \cdot v_B$). Under this case, the phase modulated sidebands will also be involved in the SBS process by the pump wave.

REFERENCES

- [1] F. Zeng and J. Yao, "Investigation of phase-modulator-based all-optical bandpass microwave filter," *J. Lightw. Technol.*, vol. 23, no. 4, pp. 1721–1728, Apr. 2005.
- [2] F. Zeng, J. Wang, and J. Yao, "All-optical microwave bandpass filter with negative coefficients based on a phase modulator and linearly chirped fiber Bragg gratings," *Opt. Lett.*, vol. 30, no. 17, pp. 2203–2205, Sept. 2005.
- [3] G. Ning, S. Aditya, P. Shum, L. H. Cheng, Y. D. Gong, and C. Lu, "Tunable photonic microwave bandpass filter using phase modulation and a chirped fiber grating in a Sagnac loop," *IEEE Photon. Technol. Lett.*, vol. 17, no. 9, pp. 1935–1937, Sept. 2005.
- [4] J. Marti, F. Ramo, V. Polo, M. Fuster, and J. L. Corral, "Millimeter-wave signal generation and harmonic upconversion through PM-IM conversion in chirped fiber gratings," *Fiber Integr. Opt.*, vol. 19, no. 2, pp. 187–198, 2000.
- [5] J. Yu, Z. Jia, L. Xu, L. Chen, T. Wang, and G.-K. Chang, "DWDM optical millimeter-wave generation for radio-over-fiber using an optical phase modulator and an optical interleaver," *IEEE Photon. Technol. Lett.*, vol. 18, no. 13, pp. 1418–1420, July 2006.
- [6] X. Zhang, H. Chi, X. Zhang, S. Zheng, X. Jin, and J. Yao, "Instantaneous microwave frequency measurement using an optical phase modulator," *IEEE Microw. Wireless Compon. Lett.*, vol. 19, no. 6, pp. 422–424, June 2009.
- [7] X. S. Yao, "Phase-to-amplitude modulation conversion using Brillouin selective sideband amplification," *IEEE Photon. Technol. Lett.*, vol. 10, no. 2, pp. 264–266, Feb. 1998.
- [8] B. Chen, S. Zheng, H. Chi, X. Zhang, and X. Jin, "An optical millimeter-wave generation technique based on phase modulation and Brillouin-assisted notch-filtering," *IEEE Photon. Technol. Lett.*, vol. 20, no. 24, pp. 2057–2059, Dec. 2008.
- [9] J. Yao, G. Maury, Y. L. Guennec, and B. Cabon, "All-optical subcarrier frequency conversion using an electrooptic phase modulator," *IEEE Photon. Technol. Lett.*, vol. 17, no. 11, pp. 2427–2429, Nov. 2005.
- [10] J. Yao, F. Zeng, and Q. Wang, "Photonic generation of ultrawideband signals," *J. Lightw. Technol.*, vol. 25, no. 11, pp. 3219–3235, Nov. 2007.
- [11] S. Wang, H. Chen, M. Xin, M. Chen, and S. Xie, "Optical ultra-wideband pulse bipolar and shape modulation based on a symmetric PM-IM conversion architecture," *Opt. Lett.*, vol. 34, no. 20, pp. 3092–3094, Oct. 2009.
- [12] H. Chi, X. Zou, and J. Yao, "Analytical models for phase-modulation-based microwave photonic systems with phase modulation to intensity modulation conversion using a dispersive device," *J. Lightw. Technol.*, vol. 27, no. 5, pp. 511–521, Mar. 2009.

- [13] Y. Ji, S. Zheng, Z. Li, X. Jin, X. Zhang, and H. Chi, "Tunable fiber Fabry-Perot filter for PM-IM conversion and efficiency improvement in radio-over-fiber links," *Microwav. Opt. Technol. Lett.*, vol. 52, no. 9, pp. 2090–2095, Sept. 2010.
- [14] G. H. Smith, D. Novak, and Z. Ahmed, "Overcoming chromatic-dispersion effects in fiber-wireless systems incorporating external modulators," *IEEE Trans. Microw. Theory Tech.*, vol. 45, no. 8, pp. 1410–1415, Aug. 1997.
- [15] R. Waarts, A. Friesem, and Y. Hefetz, "Frequency-modulated to amplitude-modulated signal conversion by a Brillouin-induced phase change in single-mode fibers," *Opt. Lett.*, vol. 13, no. 2, pp. 152–154, Feb. 1988.
- [16] A. Loayssa and F. J. Lahoz, "Broad-band RF photonic phase shifter based on stimulated Brillouin scattering and single-sideband modulation," *IEEE Photon. Technol. Lett.*, vol. 18, no. 1, pp. 208–210, Jan. 2006.
- [17] W. Li, N. H. Zhu, and L. X. Wang, "Photonic phase shifter based on wavelength dependence of Brillouin frequency shift," *IEEE Photon. Technol. Lett.*, vol. 23, no. 14, pp. 1013–1015, July 2011.

Wei Li received the Ph.D. degree in microelectronics and solid state electronics in 2010 from the Institute of Semiconductors, Chinese Academy of Sciences (CAS), Beijing, China.

Currently he is an Assistant Professor with the Institute of Semiconductors, CAS. His research interests include high-frequency characteristics of microwave optoelectronic devices, optical injection techniques, and microwave photonics.

Dr. Li won a Humboldt Research Fellowship from the Alexander von Humboldt Foundation (2011–2013).

Ning Hua Zhu (M'92) was born in Guizhou, China, on December 16, 1959. He received the B.S., M.S., and Ph.D. degrees in electronic engineering from University of Electronic Science and Technology of China, Chengdu, China, in 1982, 1986, and 1990, respectively.

From 1990 to 1994 he worked with the Electronics Department of Zhongshan University, Guangdong, China, first as a Postdoctoral Fellow, and then as an Associate Professor in 1992, and a full Professor in 1994. From 1994 to 1995, he was a Research Fellow in the Department of Electronic Engineering, City University of Hong Kong. From 1996 to 1998, he was with the Siemens Corporate Technology, Munich, Germany as a Guest Scientist (Humboldt Research Fellow), where he worked on the microwave design and testing of external waveguide modulators and laser modules. He is currently a Professor with the Institute of Semiconductors, Chinese Academy of Sciences, Beijing. In 1998 he was involved in the Hundred-Talent Program, CAS, and selected by the National Natural Science Foundation as a Distinguished Young Scientist. He founded a Joint Photonics Research Laboratory between the Institute of semiconductors, CAS and City University of Hong Kong in 1998, and served as deputy Director. His research interests are in modeling and characterization of integrated optical waveguides and coplanar transmission lines, and optimal design and testing of optoelectronic devices. He has authored over 100 journal papers and one book.

Li Xian Wang received the B.S. degree in microelectronics from Jilin University, Changchun, China, in 2006. He is currently pursuing the Ph.D. degree in physical electronics at Institute of Semiconductors, CAS, Beijing, China.

He joined the State Key Laboratory on Integrated Optoelectronics, Institute of Semiconductors, CAS, in 2006, and his current research interests are high-frequency measurement of optoelectronic devices and coherent optics.

Hui Wang was born in Shanxi, China, in 1987. He received the B.Sc. degree in the electronic science and technology from Lanzhou University, Gansu, China, in 2009, and he is currently pursuing the Ph.D. degree in microelectronics and solid state electronics at the Institute of Semiconductors, Chinese Academy of Sciences (CAS), Beijing, China.

He joined the State Key Laboratory on Integrated Optoelectronics, Institute of Semiconductors, CAS, in 2009. His current research interest is high-frequency measurement of optoelectronic devices, light injection techniques and tests of high-speed optoelectronic devices.